Turbulence-Producing Eddies in the Viscous Wall Region

A computer simulation of turbulent flow in a channel is used to detect flow patterns related to the production of Reynolds stress. It is found that quadrant 2 and quadrant 4 events possess a streaky structure in the viscous wall region and that these events can be best understood by examining the velocity field in the y-z plane. Large turbulence production in the viscous wall region is found to occur in updrafts and downdrafts associated with closed eddies. These eddies, on average, have a spanwise dimension of 50 wall units and a streamwise dimension of 400–450 wall units. They are often seen to originate from small attached eddies at the wall.

S. L. Lyons
T. J. Hanratty
Department of Chemical Engineering
University of Illinois
Urbana, IL 61801

J. B. McLaughlin
Department of Chemical Engineering
Clarkson University
Potsdam, NY 13676

Introduction

The principal theoretical problem associated with wall turbulence is the determination of how turbulence is generated and sustained, i.e., to explain how energy is transferred from the mean flow (or a pressure gradient) to the turbulence. The presence of a wall in a turbulent field puts a constraint on the flow since all velocity components are zero at the wall. Measurements of the time-averaged velocity show changes from zero to a value close to the bulk velocity in a very short distance from the wall, typically less than a millimeter. This region of large velocity change, called the viscous wall layer in this paper, is the combination of the viscous sublayer and the buffer layer, defined in the literature. Its thickness made dimensionless with the friction velocity, u^*, and the kinematic viscosity, ν, is $y = 30$–40. The behavior of the velocity field in the viscous wall region scales with these wall parameters; therefore, all velocities are made dimensionless with u^* and all lengths with the viscous wall length ν/u^*.

Early workers in the field of turbulence had thought that turbulent flow close to the wall responds passively to fluctuations in the outer flow. A contrary picture emerged from turbulence measurements in the 1950's (Hinze, 1975; Townsend, 1976). These show that both the production of turbulent energy and the dissipation of turbulent energy are quite large and of the same order in the viscous wall region. However, the difference of these two large numbers is such that there is a net positive production which supplies energy to the outer region where the local dissipation is the same (in the "log-layer") or greater (in the core) than local production.

Extensive experimental (in particular, multipoint measurements) and computational work have been done at the University of Illinois over the past 25 years to relate turbulence production in the viscous wall layer to turbulence structure. From these studies, as well as studies in other laboratories, a conceptual model has evolved, that is outlined in recent papers (Hanratty, 1989; Lyons et al., 1988; Finnicum and Hanratty, 1988).

Research on this problem has been greatly invigorated in the past five years by the successful computer calculation, from the Navier Stokes equations, of the time-varying velocity and pressure fields for fully-developed turbulent flow in a channel (Kim et al., 1987). A similar code, developed by Steve Lyons and John McLaughlin for use on the University of Illinois supercomputer, is described in a recently published thesis (Lyons, 1989).

The purpose of this paper is to use the results of this computation to identify eddy structures associated with the production of turbulence in the viscous wall layer.

Conceptual Model Suggested by Laboratory Measurements

Initial efforts in examining the results of the computations have been greatly influenced by the conceptual model that has evolved from past experimental work. Therefore, it is useful to present a brief discussion of this model.

The two structural characteristics of wall turbulence that have proved to be the most useful are: the scaling of the streaky structure close to the wall and the scaling of the log-layer. Injection of dye at the wall and various instrumental measurements have revealed elongated, organized structures in the viscous wall layer that are associated with long streaks of low velocity fluid having a spanwise spacing of $\lambda = 100$. The log-layer extends from the edge of the viscous wall region to 0.15–0.20 channel half-widths. It is a region where the mean velocity varies with

the logarithm of the distance from the wall. Prandtl has argued that the characteristic length scale of the eddies controlling the transfer of momentum varies linearly with distance from the wall in the log-layer. On the basis of correlation measurements, Townsend (1976) embellished this idea of Prandtl by describing the log-layer as being dominated by attached wall eddies (elongated in the flow direction) that increase in size linearly with distance from the wall. Townsend argued that the eddies which are the main contributor to Reynolds stress, normal velocity fluctuations and turbulence production at a given distance from the wall are the ones whose centers are close to the location being considered.

We have adopted the picture that the level of Reynolds stress and the production of turbulence in the viscous wall region can be associated with eddy motion in a plane perpendicular to the flow direction which appears intermittently close to the wall and which has an average spanwise dimension, ℓ, of about 50 wall units (Sirkar and Hanratty, 1970; Lee et al., 1974). Various measurements (Hanratty, 1989) suggest these eddies are elongated in the flow direction, having lengths six to ten times their widths. In the region $y < 15$, the wall eddies have inflows and outflows of the same strength. They thus could be pictured "on average" as coupled inflows and outflows, depicted in Figure 1. Here, λ is defined as the distance between low velocity streaks and $\ell = \lambda/2$ is the eddy size.

These eddies create streamwise velocity fluctuations, u, by bringing high momentum fluid to the wall, exchanging momentum with the wall and carrying low momentum fluid away from the wall. Since the high momentum fluid is transported by negative normal velocities, v, and low momentum fluid by positive normal velocities, these flows are associated with large values of $-uv$. They are, thus, important contributors to the Reynolds stress and to the production of turbulence. There is a temporal lag between the development of the velocity pattern associated with the eddy and the u-pattern it causes; therefore, the period over which strong Reynolds stress exists has been estimated to be less than the lifetime of the eddies.

Wall eddies with $\ell \ll 50$ do not extend to the edge of the viscous wall region, y_o, and could be looked upon as separation bubbles in the y-z plane formed by the interaction of large-scale eddies with the wall (Fortuna, 1971; Nikolaides, 1984; Hanratty, 1989). Correlation measurements and frequency-wavenumber measurements (Grant, 1958; Tritton, 1967; Nikolaides et al., 1983a, b; Nikolaides, 1984; Hogenes and Hanratty, 1982) suggest that eddies with average spanwise dimensions of about

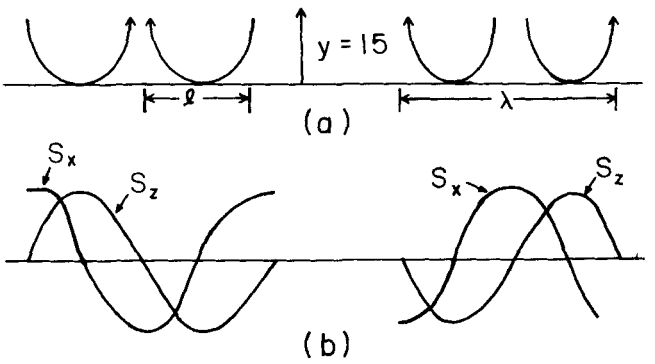

Figure 1. Wall eddies and their effect on the two components of the wall velocity gradient.

50 ($\lambda = 100$) extend through the entire viscous wall region. They can be identified close to the wall from the spanwise variation of the spanwise and streamwise velocity components and have the same spanwise scale as the normal velocity fluctuations at $y_o \approx 30$. Eddies with spanwise scales much larger than $\ell \approx 50$ can also affect the flow in the viscous wall layer. They do not seem to play a direct role in determining the Reynolds stress but they do control the level of streamwise and spanwise velocity fluctuations at y_o. Conditional sampling measurements with multiple probes (Nikolaides et al., 1983a) suggest that the $\lambda = 100$ eddies are approximately closed (that is, they have well-defined circulations in the y-z plane) and, on average, have their center below $y = 40$ during periods that Reynolds stress production is most important. The streamwise extent of these closed eddies during these periods of high activity was estimated to be 150 wall units.

Measurements with multiple wall probes (Eckelman, 1971; Lee et al., 1974) give $s_z(z)$ variations that differ from the idealized pattern in Figure 1 in that there is a distribution of wavelengths, the eddies between two updrafts can be of different size and a large eddy may contain a smaller separation bubble (in the y-z plane). They do, however, agree with the pattern suggested by Sirkar and Hanratty (1970), in which downdrafts are found, on average, to have the same strength as updrafts.

In the context of Townsend's model, the $\lambda = 100$ patterns shown in Figure 1 are associated with eddies which are strong contributors to the normal velocity and Reynolds stress in the viscous wall region and which are the smallest of any consequence in the log-layer. These eddies are the principal contributors to the spanwise velocity very close to the wall. However, larger attached eddies which are not important contributors to the Reynolds stress in the viscous wall region dominate spanwise flow in the outer part of the viscous wall region.

The results outlined above have prompted the representation of the time-varying flow in the viscous wall region by "slender body turbulence" or the "2½ D model" used by Hatziavramidis and Hanratty (1972) and by Chapman and Kuhn (1981). The main simplifications are the neglect of derivatives in the flow direction and the assumption that the flow at y_o can be described with two scales, one characterizing the wall streaks ($\lambda = 100$) and the other, the influence of large outer flow eddies (Nikolaides, 1984; Lyons et al., 1988; Finnicum and Hanratty, 1988). Calculations based on these simple models give a good representation of statistical properties of the turbulent velocity field within the viscous wall layer and agree with the experimental finding that drag-reduction is associated with an increase in λ.

Computer Simulation of Turbulent Flow

The simulation used in this paper solves the three-dimensional time-dependent Navier-Stokes equations spectrally, with a fractional-step algorithm developed by Orszag and Kells (1980) and a modification proposed by Marcus (1984). Considered here is the fully-developed turbulent channel flow at a Reynolds number of 2,260 based on the half channel height and the bulk average velocity.

The dimensions in wall units of the computational channel are as follows: the half channel height is 150; the spanwise periodicity length is 950; and the streamwise periodicity length is 1,900. The spanwise and streamwise periodicity lengths are large enough to make all velocity correlations go to zero within half of those periodicity lengths. The current simulation uses 65 Cheby-

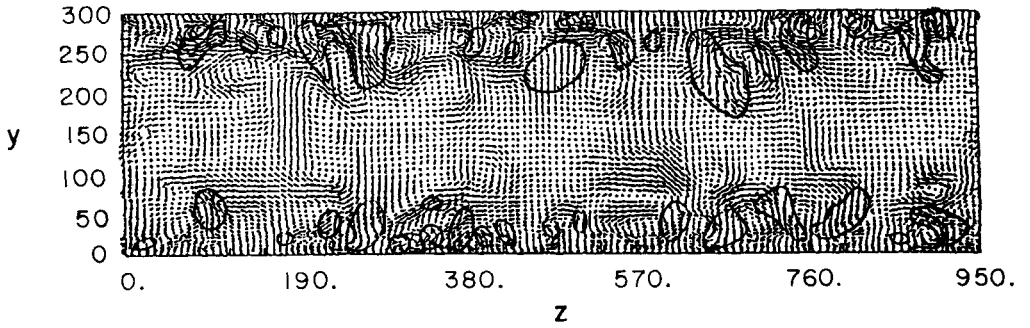

Figure 2a. Instantaneous velocity vectors in the *y-z* plane.
Regions were $-uv > 1$ are highlighted.

shev polynomials in the normal direction that give a grid spacing of 0.18 at the wall and of 7.36 in the center of the channel. Eighty-five Fourier modes are used in the spanwise direction and 85 Fourier modes, in the streamwise direction giving uniform grid spacings of 11.18 in the spanwise direction and 22.35, in the streamwise direction. The collocation points are expanded by the "three-halves" rule when transforming from spectral space to physical space during the computation of the nonlinear terms. Good agreement is obtained between the computed velocity field and measurements of the u- and v-velocity components made at the same conditions by Niederschulte (1989).

A limitation is that the computations must be done at a low Reynolds number. It is noted that 20% of the channel half width would correspond to $y = 30$. Thus, the classical log-layer, which extends from $y = 30$ to $y/a = 0.20$, does not exist.

Results

Eddy patterns in the y-z plane

Figure 2a is a picture of an instantaneous flow field showing an entire y-z plane perpendicular to the flow. The orientation of the vectors indicates the local direction of flow. The length gives the speed. The enclosed regions are where $-uv$ is roughly twice $-\overline{uv}$ ($-uv > 1$).

Turbulence production is given by $-\overline{uv}\,(d\bar{U}/dy)$ so that local instantaneous contributions to turbulence production can be calculated from $-uv(d\bar{U}/dy)$. Large values of this quantity correspond roughly to large values of $-uv$ indicated in Figure 2a. Therefore, regions with large turbulence production are identified by the enclosed spaces in Figure 2a.

The region close to the bottom wall at $500 < z < 900$ is one of large activity, so it is expanded in Figure 2b. Here, it is noted that production is largest at shear layers between enclosed eddies. The centers of these eddies are at $y \leq 40$. The spacing of the regions of intense activity between $z = 600$ and $z = 800$ is 50-70.

Reynolds stress patterns in the x-y *plane at* y = *11.4*

Since the focus was on turbulence production is the viscous wall layer, it was decided to examine in more detail the Reynolds stress patterns at the location where the production of turbulence is a maximum, $y = 11.4$. Plots of calculated distributions of $-uv$ at $y = 11.4$ are shown in Figure 3. Positive contributions to $-\overline{uv}$, identified by quadrant 2 (positive v, negative u) and quadrant 4 (negative v, positive u) events, contribute 116.8% while positive uv events contribute -16.8%. Quadrant 2 (outflow) and quadrant 4 (inflow) events become equal contributors to $-uv$ at $y = 14$ with quadrant 4 contributing more for $y < 14$ and quadrant 2 contributing more for $y > 14$. This agrees with Figure 16 in Kim et al. (1987).

Figure 3 gives the fraction of the Reynolds stress contributed by uv magnitudes lower than some threshold value $(uv)^*$. Since dimensionless $-\overline{uv} = 0.44$ at $y = 11.4$ it is seen that only about 7% of the Reynolds stress is contributed by events having magni-

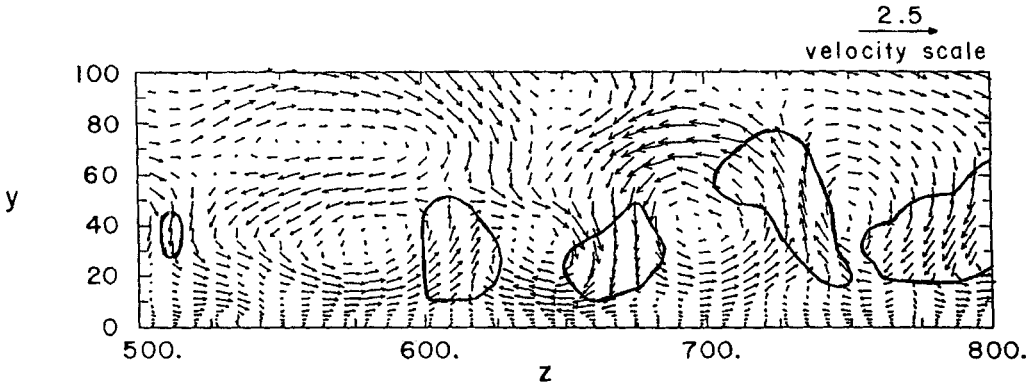

Figure 2b. Expansion of figure 2a showing instantaneous vectors in the *y-z* plane.
Regions were $-uv > 1$ are highlighted.

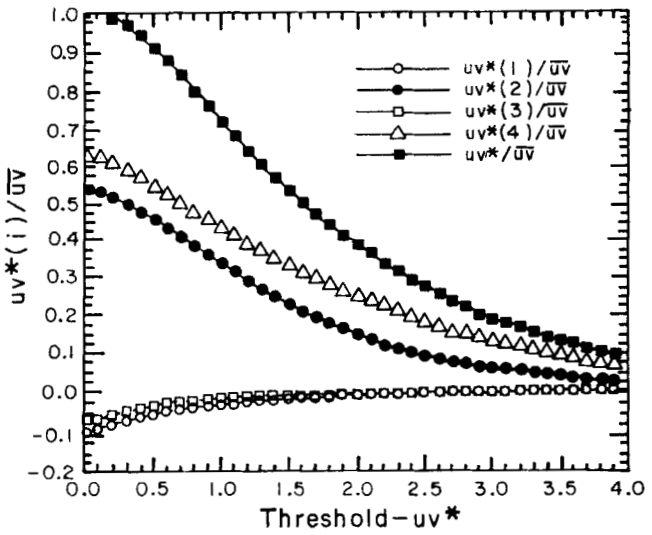

Figure 3. Distribution of Reynolds stress at $y = 11.4$.

tudes equal to or less than $-\overline{uv}$. The events encircled in Figure 2 have $-uv^* > 1$. From Figure 3 it is indicated they contribute about 70% of the total Reynolds stress at $y = 11.4$.

Figure 4a shows all of the quadrant 2 events at $y = 11.4$ at a given instant of time as vectors showing the direction and magnitude of flow in the x-z plane. These show a streaky structure similar to what is observed when dye is injected at the wall. The spanwise spacings and lengths of the streaks are roughly of the order of 100 and 1,000. However, it is noted that the coherency in the flow direction is smaller if the flow field were followed at a constant value of z. The same type streaky structure is found for negative u.

It is noted that in some cases the quadrant 2 streaks divide to form pocket-like spaces, terminate or suddenly change directions. These most often are locations where a quadrant 2 event is just upstream of a quadrant 4 event or where there is sudden change from a negative to a positive streamwise velocity. There are also instances in which quadrant 2 events initiate or join, or where quadrant 4 streaks change direction. These are locations where there is a sudden change from a positive streamwise velocity to a negative streamwise velocity. They seem to represent the structure captured by Adrian et al. (1987). (See figure 12 of their paper.)

Figure 5a shows quadrant 2 events with values of $-uv$ greater than 0.8. For this threshold, negative contributions to Reynolds stress are negligible. Roughly 80% of the contribution to Reynolds stress by quadrant 2 events and 1/3 of the total quadrant 2 events are captured. The streaky structure observed is much clearer than indicated in Figure 4a where all the quadrant 2 events are shown.

Figure 4b shows all of the quadrant 4 events and Figure 5b shows events using a threshold which captures the same fraction of the quadrant 4 contribution to Reynolds stress at $y = 11.4$ as does Figure 5a for the quadrant 2 contribution. A streaky structure is noted, but the streaks are broader and stubbier than the quadrant 2 events.

Eddy patterns in the y-z *plane associated with* uv *streaky structure at* y = *11.4*

Figures 6-8 show typical eddy patterns in the y-z plane associated with Reynolds stress production at $y = 11.4$. These figures are at the same computational time as Figures 4–5 and regions where $-uv > 0.85$, $y = 11.4$ are highlighted. One can see immediately that Reynolds stress production at $y = 11.4$ can be associated with inflows and outflows caused by roller (approximately closed) eddies in the y-z plane.

A quadrant 4 streak at $z \approx 550$ and a quadrant 2 streak at $z \approx 600$ are associated with an eddy which pairs asymmetrically with an eddy on the right in Figures 6a and 6b, and on the left for figures 6c, 7 and 8a. These eddies interact to create an inflow

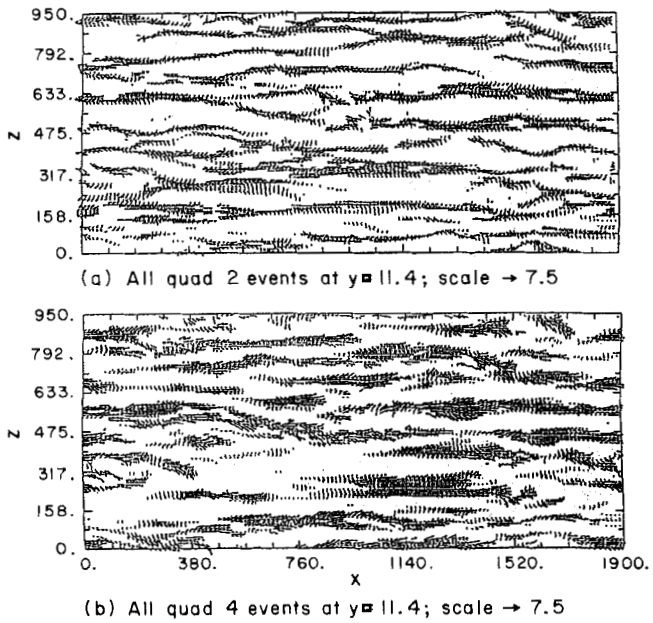

Figure 4. All of the quadrant 2 and quadrant 4 Reynolds stress events in the x-z plane at $y = 11.4$.

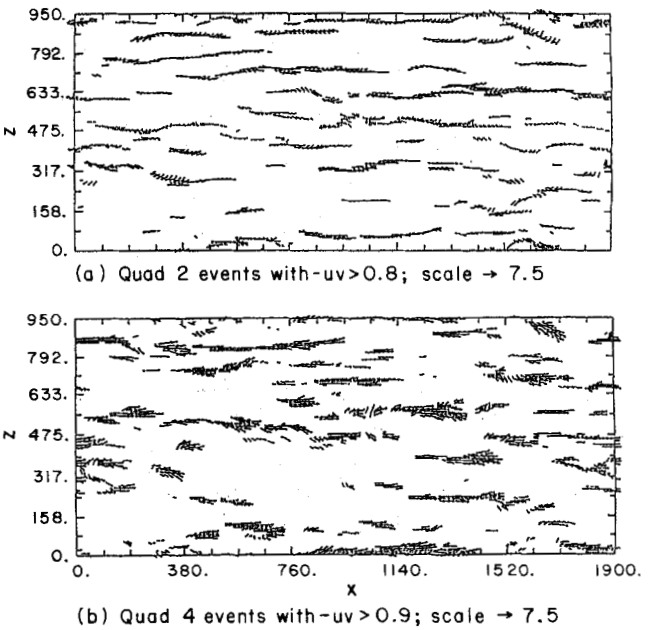

Figure 5. Events in the x-z plane at $y = 11.4$ that represent 80% of the Reynolds stress contributed by quadrant 2 and by quadrant 4 events.

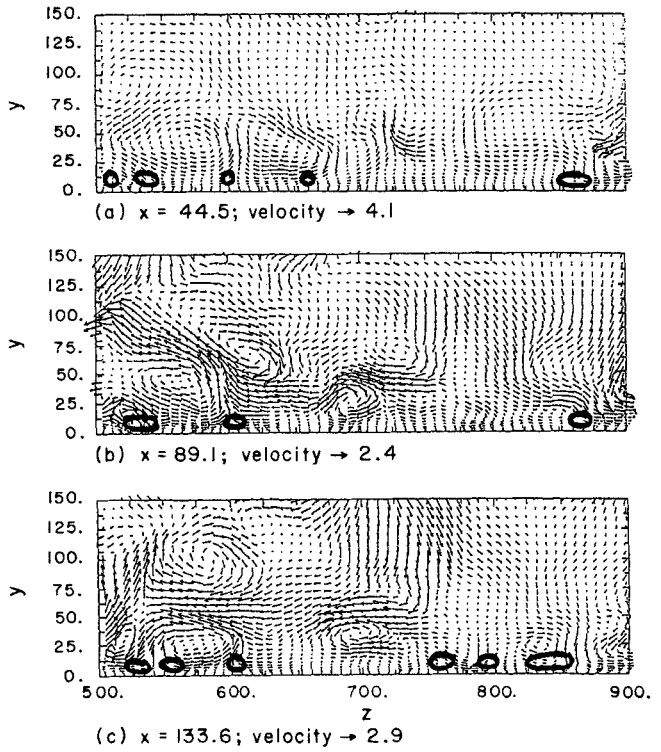

Figure 6. Instantaneous flow patterns in the *y-z* plane at $x = 44.5, 89.1, 133.6$.

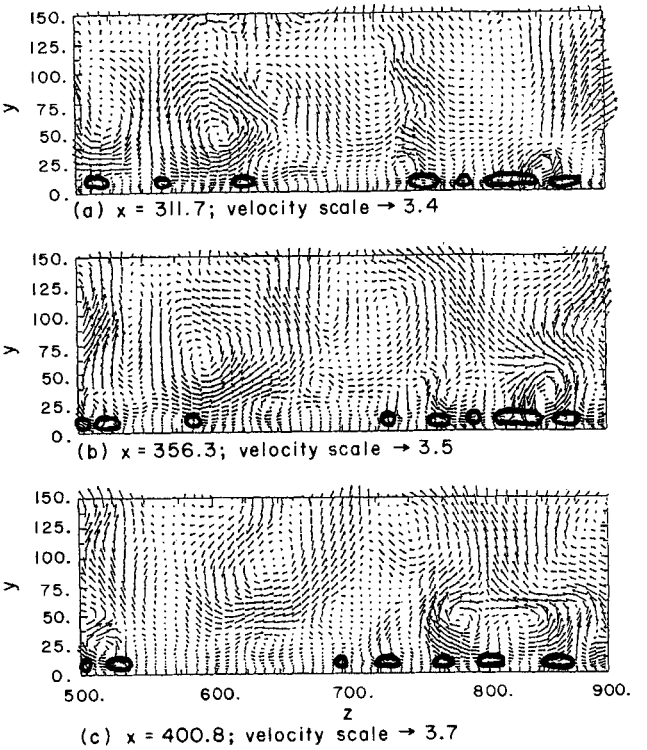

Figure 8. Instantaneous flow patterns in the *y-z* plane at $x = 311.7, 356.3, 400.8$.

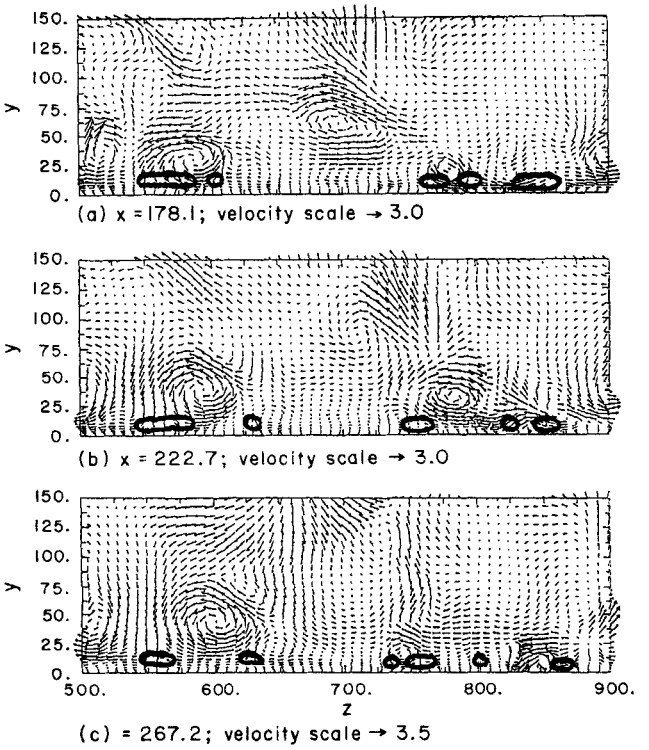

Figure 7. Instantaneous flow patterns in the *y-z* plane at $x = 178.1, 222.7, 267.2$.

at $z \cong 550$ and an outflow at $z \cong 600$ forming two uv streaks in the x-z plane from $x = 44.5$ in Figure 6a through $x = 311.7$ in Figure 8a (see Figures 4 and 5). Note that in Figures 7b through 8b these eddies can be seen to lift from the wall and grow in size as they progress downstream.

Another interesting sequence of events is shown in Figures 7a–8c, where a Reynolds stress producing eddy is created at the wall at $z = 850$. A large spanwise flow at the wall causes the spanwise shear layer at the wall to lift and give the appearance of a separation bubble in the y-z plane (Figures 7a and 7b). This separation bubble grows as it progresses downstream by entraining fluid and far enough downstream lifts from the wall as shown in Figures 8b and 8c.

Figures 6–8 show the typical sequence of events in the creation of the Reynolds stress streaky structure in the viscous wall region. Eddies appear to originate at the wall where they interact to form inflows and outflows. These inflows and outflows persist for several hundred wall units in the x-direction bringing high and low streamwise momentum fluid to and from the wall, creating quadrant 4 and 2 Reynolds stress events. Downstream, the eddies lift from the wall and grow in size to become outer flow eddies.

Conditionally-averaged eddy structure

The average size of the eddies associated with turbulence production in the viscous wall region was obtained by conditionally averaging on all values of quadrant 2 or quadrant 4 events larger than a selected threshold at $y = 11.4$. (Thus, if the conditional averaging were triggered on quadrant 2 events with $-uv > 0.8$, the velocity field would be averaged around all of the vectors shown in Figure 5a). Figure 9b shows the average vector field in

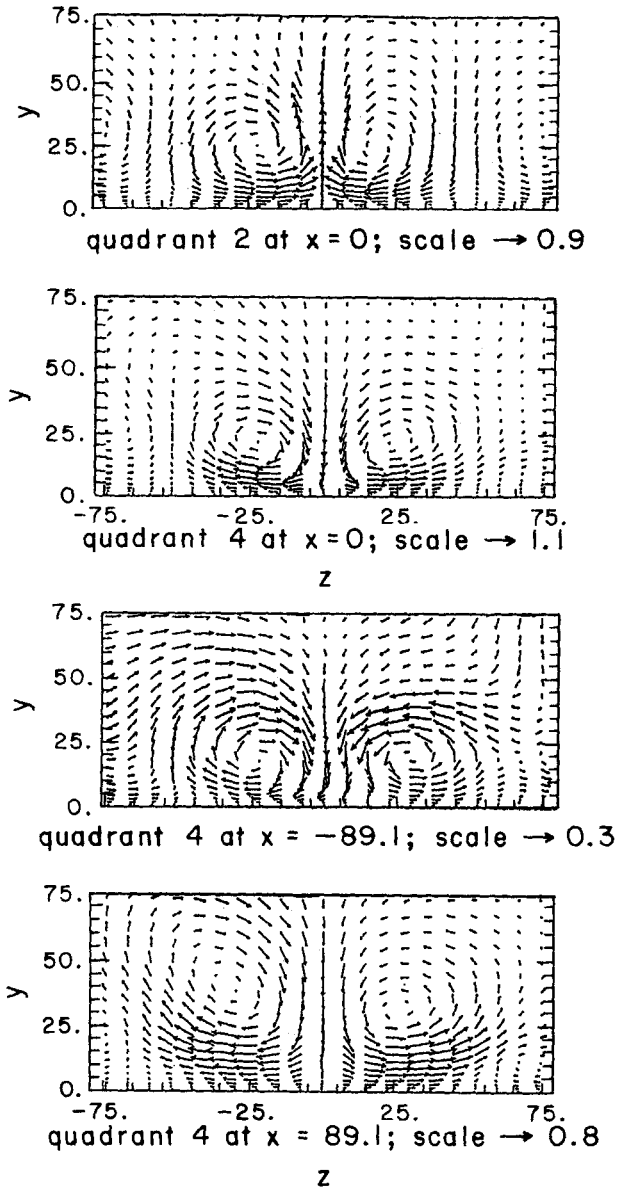

Figure 9. Flow pattern in the *y-z* plane at $x = 0$, $x = -89.1$, $x = +89.1$, conditionally sampled for quadrant 2 event [$-uv$ ($x = 0$, $y = 11.4$, z) > 1.3, $v > 0$] and quadrant 4 event [$-uv(x = 0, y = 11.4, z) > 1.6$, $v < 0$].

the y-z plane of the 867 quadrant 4 (inflow) events with $-uv > 1.6$ at $y = 11.4$, $z = 0$. This threshold was chosen so as to account for 50% of the contribution of quadrant 4 events to the Reynolds stress. Such events occurred 5% of the time. Figure 9a shows the average of 966 quadrant 2 events for which $-uv > 1.3$. These occurred 5.4% of the time and accounted for 50% of the contribution of quadrant 2 events to the Reynolds stress.

These patterns seem insensitive to the choice of a threshold value. For example, thresholds of $-uv > 0.4$, 0.9, 2.5 and 4.1, corresponding to 90, 70, 30 and 10% of the quadrant 4 events, gave eddies of the same size as shown in Figure 9. However, the v- and u-kinetic energies of these eddies differed. It is to be noted that the choice of a higher threshold, such as $-uv > 4.1$, has the effect of centering the conditional average in the structure being studied [as was done by Johansson et al. (1987) in their study of shear layer structures in a channel flow].

Instantaneous eddy patterns of the type shown in Figures 6–8 indicate that updrafts and downdrafts, associated with eddies having a range of sizes, are contributors to the $-uv$ product. Furthermore, these eddies usually pair with another eddy of a different size. Therefore, the conditional eddies shown in Figure 9 are an average representation and the symmetry is an artifact of the method of averaging (Guezennec et al., 1987). It is noted that the eddies representing conditionally averaged quadrant 2 and quadrant 4 events are roughly the same size. They extend through the viscous wall region and have spanwise dimensions of 50. The centers of the quadrant 4 and quadrant 2 eddies are respectively located at $z = \pm 25$, $y = 22$ and at $z = \pm 20$, $y = 25$.

Figure 10a is the turbulent flow in the x-z plane at $y = 11.4$ conditionally averaged for quadrant 4 events with $-uv > 1.6$ at $x = 0$, $z = 0$. It is consistent with the structure indicated in Figures 4 and 9. The pattern has a streak of positive velocity at $z = 0$ and two streaks of negative velocity at $z = \pm 50$. Its length is greater than 450 wall units. Figure 10b shows the turbulent pattern in the y-x plane conditionally averaged for quadrant 4 events with $-uv > 1.6$ at $y = 11.4$, $x = 0$. This shows a downflow of high momentum fluid to the wall over an extended region in the flow direction. Figure 11a shows Reynolds stresses in the x-y plane that are conditionally averaged for a quadrant 4 event with $-uv > 1.6$ at $y = 11.4$. The region of high $-uv$ is seen to be of smaller extent (about 325 wall units) than the conditionally sampled flow patterns in Figure 10. Note that the vertical scale in Figure 11 (as well as in 12–17) is stretched in order to expand the viscous wall region.

Figure 10 can be interpreted if one pictures the eddies in Figure 9b bringing high momentum fluid toward the wall at $z = 0$ and bringing low momentum fluid away from the wall at $z = \pm 50$. The high momentum region at $z = 0$ appears to extend farther in the region $x < 0$ than in the region $x > 0$.

The conditionally-averaged velocity fields in Figures 9 and 10 show that w is zero at $z = 0$ and is a maximum at $z = 22.3$.

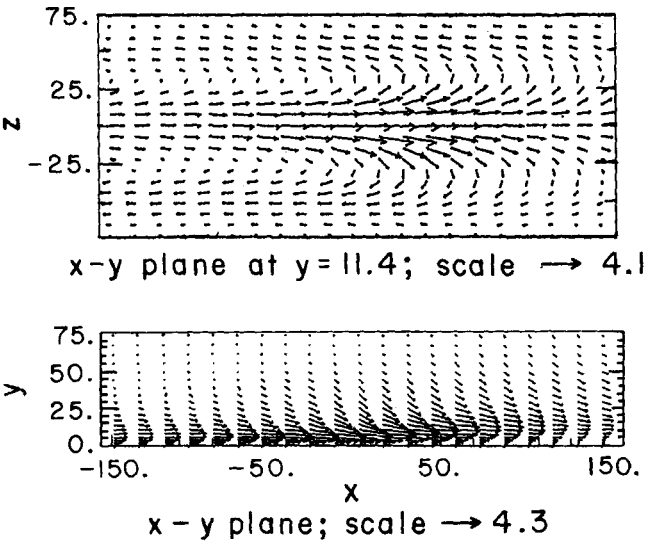

Figure 10. Conditionally sampled flow pattern in *x-z* plane at $y = 11.4$ and in the *y-x* plane at $z = 0$ for a quadrant 4 event [$-uv(x, y = 11.4, z) > 1.6$, $v < 0$].

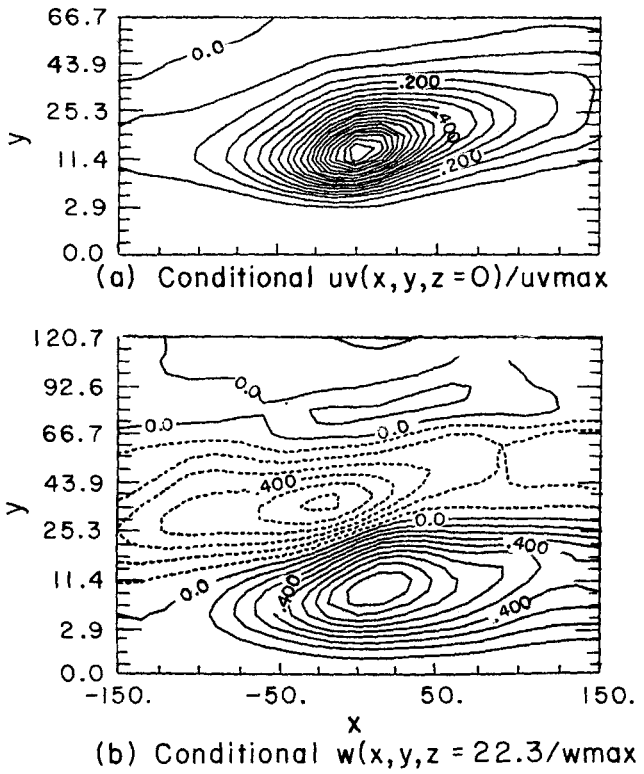

Figure 11. Contours of Reynolds stress (normalized by $-uv = 3.01$) at $z = 0$ and spanwise velocity (normalized by $w = 0.756$) at $z = 22.3$ in the y-x plane at $z = 0$ for quadrant 4 event $[-uv(x = 0, y = 11.4, z = 0) > 1.6, v > 0]$.

Therefore, the w velocity field at $z = 22.3$ was conditionally averaged for strong quadrant 4 events at $z = 0$, $y = 11.4$. As shown in Figure 11b, the maximum spanwise velocity, equal to 0.756, occurs at $x \approx 15$ and $y \approx 9$. A minimum occurs at $x \approx -20$ and $y \approx 36$. This can be interpreted as suggesting an eddy attached to the wall with its plane of circulation tilted at an angle of 45° or as an eddy moving away from the wall at an angle of 45°.

An examination of vector diagrams of the type shown in Figures 6–8 at different x seem to suggest that the eddies are formed at the wall by large-scale spanwise velocities and that they grow in size as they move away from the wall. This receives some support from conditionally-averaged velocity fields upstream and downstream of the detection point ($x = 0$, $z = 0$, $y = 11.4$) for quadrant four events. Figures 9c and 9d show conditionally-averaged flow patterns in the y-z plane at $x = -89.1$ and at $x = +89.1$. A comparison with Figures 9a and 9b shows that eddy patterns at $x = -89.1$ and at $x = 0$ are approximately the same. However, at $x = +89.1$ the eddies have lifted from the wall and increased in size.

Flow fields conditionally averaged for quadrant 2 events at 11.4 yield about the same information as given in Figures 9–11, so they are not presented here. The thesis by Lyons (1989) can be consulted for these results.

Conventional correlations

The picture presented in the previous section from conditionally-averaged velocity fields is supported by calculations of conventional correlations. Kim et al. (1987) presented spatial correlations of the u, v and w velocities at $y = 5.39$, 10.52, 149.23. Circelli and McLaughlin (1988) reported spatial correlations and wavenumber spectra for u, v, w and uv at $y = 5.39$, 46.6, 80 calculated with the NASA Ames code. The results in this section extend these works so as to include other correlations with a larger range of y and confirm the results presented in these previous papers.

Figure 12a gives the correlation between the u-velocity and the v-velocity at fixed y, $\overline{u(y, 0)\, v(y, z)}$. Here, u' and v' signify the root-mean square of the u- and v-velocity fluctions. The dashed contours are constant negative values and the solid contours are positive values. These contours indicate that at any fixed y the fluctuations of u at $z = 0$ are related to fluctuations of v of the opposite sign for small z. However, at large z the corre-

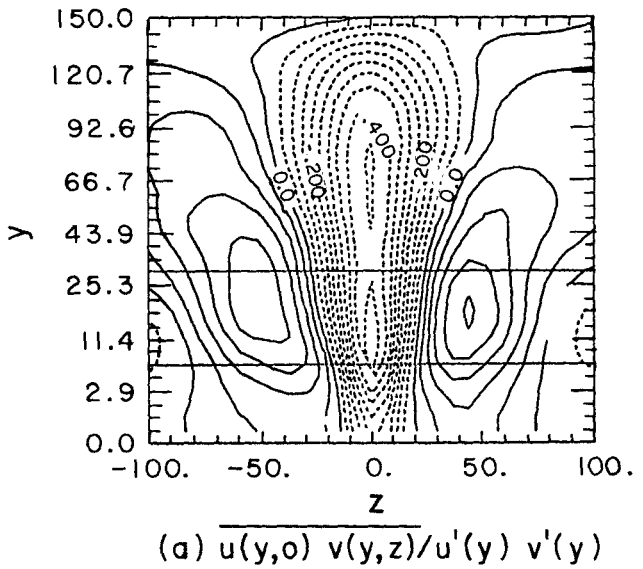

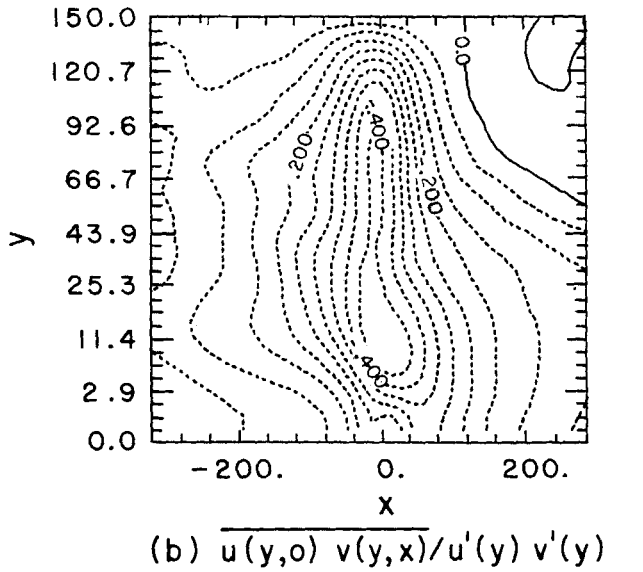

Figure 12. Two-point cross-correlations of u and v at fixed y and different separations in the x and z-direction.

The two horizontal lines represent $6.5 < y < 29.5$.

lation changes sign, so the opposite is true. The size of eddies, ℓ, at fixed y that are creating u-fluctuations can be defined as the distance between the maximum negative value at $z = 0$ and the maximum positive value or as two times the value of z at which a zero crossing occurs. It is noted that the spanwise dimension of eddies defined in this way increases with increasing y. The sublayer region of $y < 6.5$ has an $\ell \cong 40$. The region $6.5 < y < 30$, where the principal influence of Reynolds stress in the viscous wall region occurs, is indicated by the two horizontal lines. It is noted that the eddies in this region are roughly characterized by a dimension $\ell = 50$ (or $\lambda = 100$). The size of the eddies contributing to the Reynolds stress in the center regions of the channel are about twice the size of those in the viscous wall layer, $\ell \cong 100$.

Correlations between u and v at fixed y, but with spatial separations in the x-direction are shown in Figure 12b. The definition of an eddy size is not so clearcut. The extent of a stress producing event in the x-direction is (arbitrarily) defined as the extent of the region encompassed by the contour defining a correlation coefficient of -0.1. Thus, an estimated length of 450^+–500^+ is obtained, indicating that the stress producing events have length to width ratio of 9–10. This ratio decreases in the core of the channel to a value of 2–3.

Correlations between u and w velocity components are shown in Figure 13a. At $z = 0$, this correlation is zero because of symmetry in the z-direction. Well organized structures are suggested only for $y < 25.3$. It is noted that positive streamwise velocity fluctuations at $z = 0$ are associated with positive w-velocities at $z > 0$ (positive correlations) and negative w-velocities at $z < 0$ (negative correlations). This is consistent with the sketch in Figure 1. The opposite is the case for negative streamwise velocities at $z = 0$. Thus, an eddy size can be defined as the distance (at fixed y) between two zero contour curves or as twice the distance between the maxima and minima that exist on both sides of the $z = 0$ axis. For $y < 15$, an eddy length of $\ell \cong 50$ is estimated. Thus, the uw correlation for $y < 15$ is a good signature of the $\lambda = 100$ eddies that are producing Reynolds stress in the viscous wall region.

It is noted that for $y > 15$ u-fluctuations at $z = 0$ are strongly influenced by larger-scale w-velocities. This becomes particularly evident for $y \cong 20$. Only the bottom parts of the conditional eddies shown in Figure 9 are detected from these correlations, so observations (of the type shown in Figure 2) that large Reynolds stresses are often associated with approximately closed eddies cannot be deduced from Figure 13a.

The $v(y, 0)$ $w(y, z)$ correlation coefficients shown in Figure 13b represent properties of eddies in the y-z plane, such as depicted in Figure 2. It is noted for $y < 6.5$ that a minimum and a maximum occur at $z = \pm 15$ and that zero crossings are separated by a distance of $z \cong 50$. This suggests a range of eddy sizes from $\ell = 30$ to $\ell = 50$ in the viscous sublayer. The conditional eddies shown in Figure 9 have centers at $y \cong 20$–25. It is clear from a consideration of Figure 9 that vw correlations at $y \cong 20$ would not be a good means of detection (since the conditionally averaged w is zero at $y \cong 20$). This is borne out in Figure 13b where it is noted that the vw correlation is affected by large-scale w fluctuations (as is also indicated in Figure 13a for u fluctuations). The change in sign of the vw correlation with increasing y at a fixed value of z suggest the existence of closed counter-rotating eddies roughly centered at $y \cong 40$.

The presence of closed eddies in the viscous wall region is best

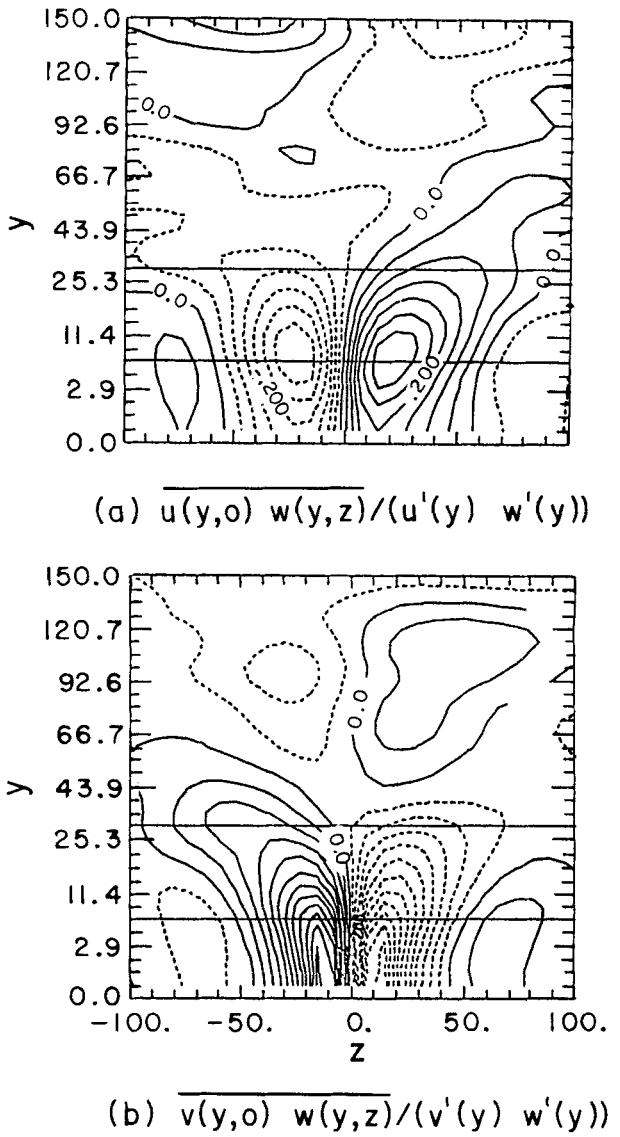

Figure 13. Two-point correlations of u at $z = 0$ with v at z and of v at $z = 0$ with w at z for different fixed y.

The horizontal lines indicate $6.5 < y < 29.5$.

exhibited by the correlation shown in Figure 14c. It was inferred from the results in Figure 13a that the $\lambda = 100$ eddies producing Reynolds stress in the viscous wall region can be associated with spanwise velocity fluctuations at $y = 6.5$. Therefore, correlations were calculated in the y-z plane between $w(y = 6.5, z = 0)$ and $w(y, z)$. Eddy structures of the type shown in Figure 9 are suggested. As can be seen in Figure 14c, there is a change in sign of the correlation at $y = 25$ and $z = 0$. This roughly corresponds to the center of the conditional eddies shown in Figure 9. The pairing of eddies is also suggested by the presence of minima in the correlation at $y = 6.5$ at $z = \pm 50$.

The existence of a streaky structure throughout the viscous wall region is indicated in Figure 14a, where the correlation between $u(y = 6.5, z = 0)$ and $u(y, z)$ is presented. Alternating regions of positive and negative correlation with spanwise separations of 50 are noted. A comparison of Figures 14a and 14c

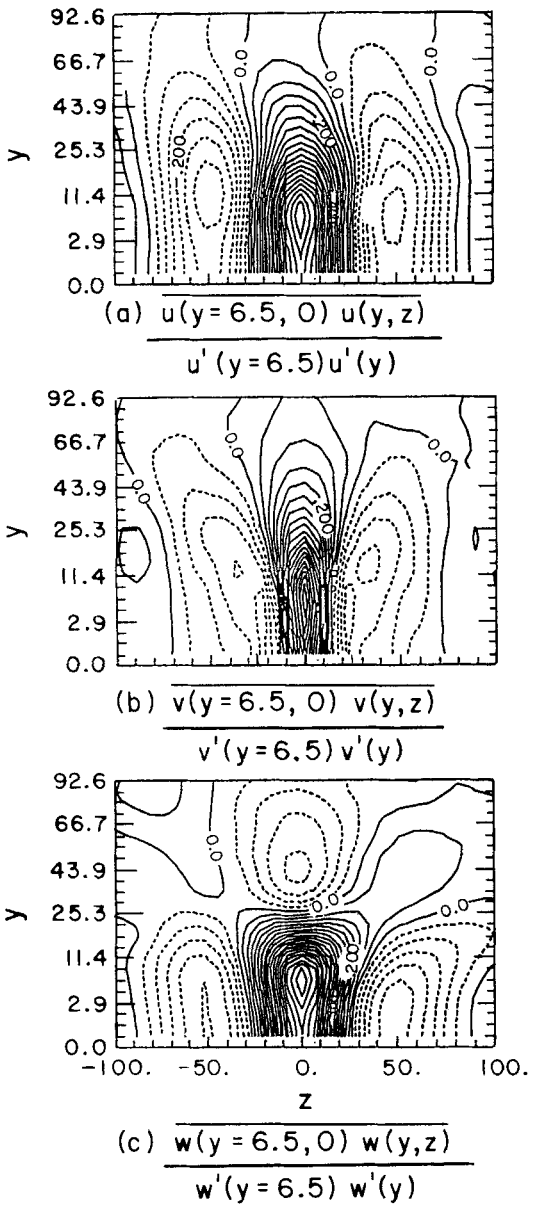

Figure 14. Two-dimensional two-point cross-correlations of a velocity component at $z = 0$, $y = 6.5$ and the same velocity component at y and z.

supports the notion that streaks of low-velocity fluid are created close to the wall by the convection of velocity deficient fluid through spanwise velocity fluctuations.

Figure 14b gives the correlation between $v(y = 6.5, z = 0)$ and $v(y, z)$. As already indicated in Figure 13b the v velocity at $y = 6.5$ is not a good detector of the $\lambda = 100$ eddies, since it seems to be affected by eddies with a range of sizes and, in particular, by eddies with smaller dimensions than $\ell = 50$. It is noted that, at the outer edge of the viscous wall region $y = 30$–40, the correlation shows zero crossing at $z \cong \pm 25$ and minima at $z \cong \pm 50$, indicating that the normal velocities at $y = 6.5$ are being affected (but not controlled) by well-defined closed eddies with $\ell \cong 50$. This suggests that the $\lambda = 100$ eddies are affecting v-velocities throughout the viscous wall layer, but the signature of these eddies is better given by the spanwise variation of the normal velocities at $y \cong 30$–40 rather than at $y = 6.5$.

Spatial correlations of the u, v, w velocities at fixed y are presented in Figure 15 for separations in the z-direction and in Figure 16 for separations in the x-direction. Kim et al. (1987) and Circelli and McLaughlin (1988) have pointed out that different scales characterize the spatial variation of the three components of the velocity and that this scaling can vary with distance from the wall. This is documented in the results presented in this paper. In Figure 15 it is noted that the u-correlations in the region $y < 15$ have minima at $z = 50$, and zero crossings close to 25, suggesting that $\ell = 50$ (or $\lambda = 100$) eddies are controlling streamwise velocity fluctuations in this region. At the edge of the viscous wall layer ($y = 30$–40) a characteristic eddy length of $\ell \cong 60$–70 is obtained [as had been shown earlier by Kim et al. (1987) and by Smith and Metzler (1983)]. At larger y, the minima in the u-correlations are not easily identified so the length ℓ

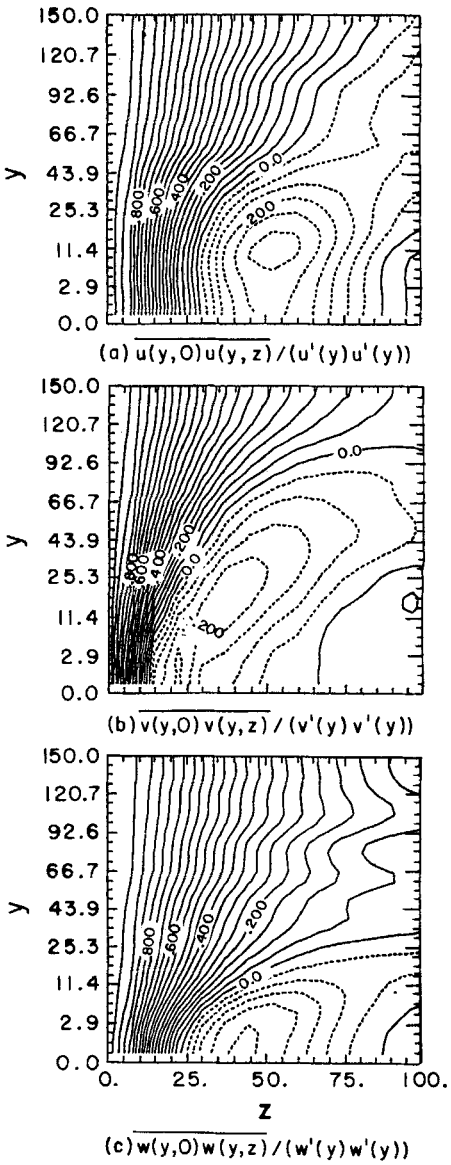

Figure 15. Two-point correlations at fixed y for different separations in the spanwise direction.

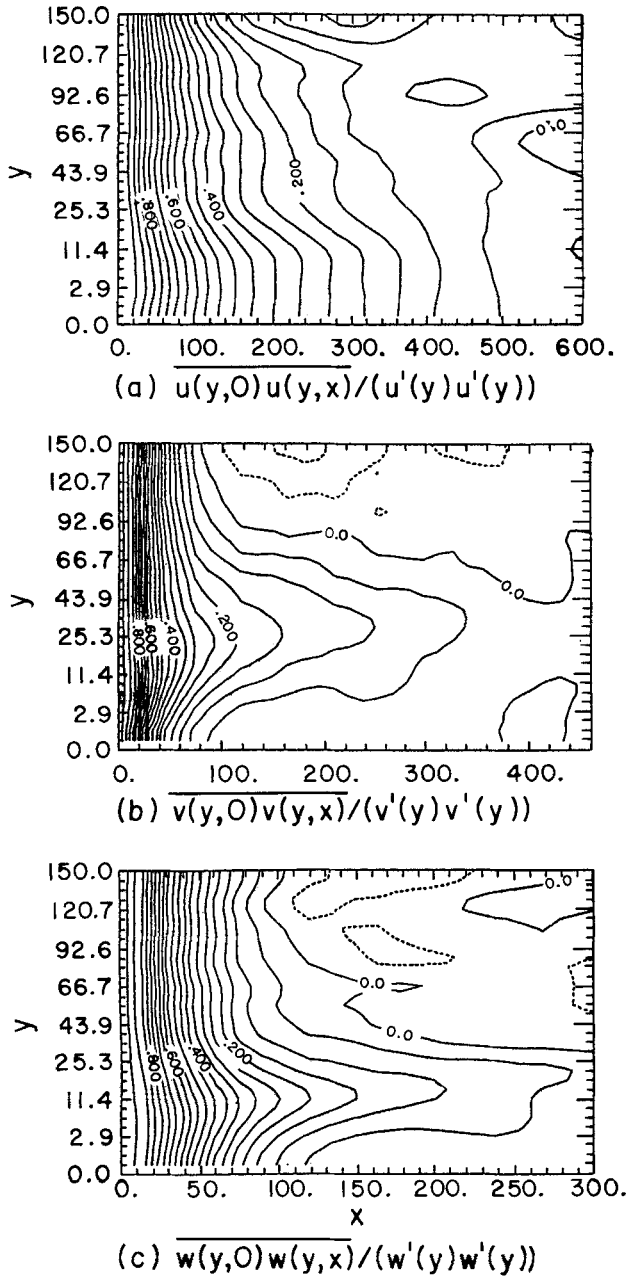

Figure 16. Two-point correlations at fixed y for different separations in the flow direction.

is defined (arbitrarily) as twice the z at which the correlation reaches a value of 0.1. This gives spanwise lengths of the eddies in the core of 100–140 wall units.

Lengths characterizing the extent of the u-velocities in the flow direction can be defined from Figure 16a as twice the value of x at which the correlation coefficient equals 0.1. In the viscous wall region a characteristic length of about 800 is obtained. It is noted that this is about twice the length of the Reynolds stress producing eddies, that are defined from Figure 10. In the core region, these streamwise lengths decrease to a value of 400–600.

Spatial correlations of w, shown in Figure 15c, indicate an eddy scale in the z-direction of $\ell = 45$–50 in the region $y < 6.3$. This increases to $\ell \simeq 70$ at $y = 11.4$ and is not well defined for larger y. A characteristic length (defined as twice the value of z at which the correlation coefficient falls to 0.1) of 110–150 is estimated for the region from the outer edge of the viscous wall layer to the channel center. The dominant feature of the spatial correlations of w in the x-direction (Figure 16c) is the extended region of high correlation in the neighborhood of $y = 11.4$. A length in the flow direction equal to that for the stress producing events, about 400, is estimated from spatial correlations shown in Figure 16c. From the outer edge of the viscous wall region to the center of the channel the extent of correlated regions of w-fluctuations is estimated as about 180.

The spatial correlations of v, shown in Figure 15b, differ from the correlations of w (in Figure 15c) in that they appear to be associated with well defined eddies for much larger distances from the wall. They show a zero crossing at $z \approx 13$ and a minimum at $z \approx 23$ in the viscous sublayer ($y < 5$). This is consistent with the observation of a maximum and minimum in the vw correlation at $z \approx \pm 13$ in the region $y < 5$. These suggest that the calculated v-velocities in the viscous sublayer are mainly associated with eddies having a dimension of $\ell \approx 25$. An examination of calculated vector diagrams of the type shown in Figures 6–8 indicate that roller eddies of this dimension appear intermittently in the region $y < 20$. Kim et al. (1987) had previously identified such structures and suggested they are streamwise vortices. The size of the eddies with which the v-velocities are associated increases with distance from the wall, so that at $y = 11.4$ length $\ell \simeq 35$, at $y = 25.3$ length $\ell \simeq 45$, and at $y \simeq 70$ length $\ell \simeq 90$. Beyond $y = 70$, the eddies are not well defined. A comparison with Figure 15c indicates that v and w-fluctuations have approximately the same extents in the z-direction at the center of the channel.

The spatial correlations of v-velocities in the x-direction, shown in Figure 16b, have a behavior similar to that of the w-velocities in Figure 16c. A maximum extent, approximately the same as the stress producing eddies, is exhibited at $y = 20$–40. In the channel core this decreases to a value similar to what is observed for the w-velocity.

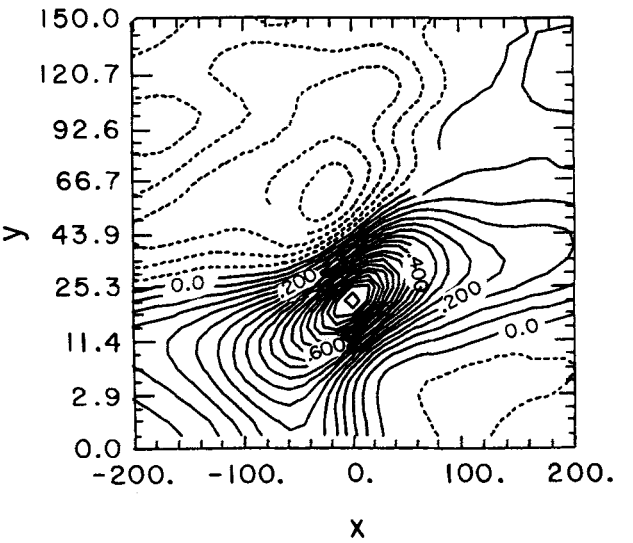

Figure 17. Two-dimensional two-point cross-correlation coefficients of $w(y = 21.3, x = 0)$ with $w(y, x)$. The contour interval is 0.05.

Evidence for the existence of tilted eddies is also obtained from correlation coefficients. Figure 17 shows the correlation between $w(y = 21.3, x = 0)$ and $w(y, x)$. The change of sign with increasing y indicates a closed eddy with its center at $y = 40$, $x = -14$. A maximum negative correlation exists at $y = 61$ and $x = -27$. This indicates that the plane of circulation of eddies centered roughly at edge of the viscous wall layer is tilted at an angle of 35°. This is consistent with the measurement presented in Figure 11 which are representing eddies closer to the wall.

Conclusions

Accuracy of computer calculations

As mentioned earlier, the computer calculations were compared with recently obtained velocity measurements in a channel at roughly the same conditions (Niederschulte, 1988; Lyons, 1989). Excellent agreement was observed for the mean velocity, the mean-square of the v velocity component and the Reynolds stress. The calculated mean-square of the streamwise velocities were about 10% lower than the measurements. This difference was believed to be real and could be a consequence of not using enough Fourier modes in the flow direction or of using a computational box which is too small. Good agreement was noted between the computed and measured flatness and skewness of the u-velocities over the whole channel and of the v-velocities only for $y > 30$.

Very large flatness factors for the v-velocity are calculated close to the wall, which had not been observed in experiments. An examination of the calculated vector diagrams suggests that these large flatnesses could be associated with the intermittent appearance of small eddies close to the wall which create large normal velocities. It is quite possible that some of the signal smoothing procedures (such as used by Niederschulte) or the large size of probes used in experiments made it difficult to capture the behavior of these small eddies. However, it is also possible that there are errors in the computer calculations.

It is noted that the dimension of the smallest eddies close to the wall ($\ell \simeq 25$) is close to the effective grid spacing of 11.13 wall units in the spanwise direction. This raises the question as to whether these small eddies are an artifact of the calculations, or whether smaller eddies would be calculated if more Fourier modes in the z-direction were used.

Clearly, calculations with better resolution are needed, but there are a number of results that seem to suggest that these small eddies are physical and close to the size of the smallest closed eddies that exist: Kim et al. (1987) used effective grid spacings of $\Delta z = 7.1$ and $\Delta z = 8.8$ and found no difference in the calculations. More importantly, their calculated correlation coefficient for v-velocities at $y = 5.39$ and $\Delta z = 7$ (Figure 2b in their paper) agrees very closely with results presented in this paper, using a grid spacing of $\Delta z = 11.13$.

Measurements have been made by Eckelman (Eckelman, 1971; Lee et al., 1974; Hanratty, 1989) of the z-component of the velocity gradient at multiple locations on the wall. From these, an eddy size can be defined as the distance between zero crossings, as indicated in Figure 1. A large number of eddies with $\ell \leq 25$ were detected in this way.

Computer simulations of the viscous wall region using a 2½ D model have also shown the existence of small closed eddies with $\ell \simeq 25$ (Fortuna, 1971; Nikolaides, 1984; Hanratty, 1989).

These type considerations lead to the conclusion that $\ell \simeq 25$ eddies predicted by the computer simulations do exist. Closed eddies smaller than $\ell \simeq 25$ also could exist. They probably would not make an important contribution to the statistical properties of the velocity field, but could represent an earlier stage in the development of the $\ell \simeq 25$ eddies.

Stress-producing events in the viscous wall layer

It has been recognized for some time that long streaks of low velocity fluid with a spanwise spacing of $\lambda \simeq 100$ exist in the viscous wall layer. This paper shows that quadrant two (outflow) or quadrant four (inflow) Reynolds stresses also have streaky structures and that the same eddies responsible for creating the streaks of low velocity fluid also create Reynolds stresses in the viscous wall layer ($y < 30$–40).

There seems to be some differences in the literature on this point. These arise from differences in the threshold used to define a stress producing event. For example, Robinson et al. (1988) used $|u'v'| > 2.6$ to detect large stress producing events at $y = 15$. These would account for only about 20% of the total stress and appear in localized regions in Figure 9 of their paper. On the other hand, Kim and Spalart (1987) display a localized streaky structure for quadrant 2 events using $|u'v'| > 0.44$ at $y = 12$.

By examining conditionally-averaged flows associated with quadrant 2 or quadrant 4 Reynolds stress events *at the location* of maximum turbulence production ($y = 11.4$), it is found that the physics of the process is best understood by examining eddy patterns in the y-z plane. Turbulence production is found to be associated (*on average*) with approximately closed eddies (roller eddies) in this plane, whose center is located at $y = 20$–25, and whose spanwise dimension is approximately 50. The size of the eddies in the y-z plane does not appear extremely sensitive to the level of uv chosen to identify Reynolds stress events, but the extent in the flow direction does. Correlation measurements indicate the organized stress producing eddies are slightly elongated in the flow direction, having lengths of 450–500.

Even though the main stress producing event appears to be represented by an average eddy of the same size throughout the viscous wall layer, the fluctuating flow cannot be characterized by a single scale. Organized eddies, which increase in average size with distance from the wall, are the main contributors to normal velocities. Close to the wall in the viscous sublayer they are controlled by eddies with $\ell = 20$–25 and at the outer part of the viscous wall layer ($y = 20$–40), by the same eddies that are the main contributor to the Reynolds stress. The organized Reynolds stress producing eddies control the spanwise velocity fluctuations only for $y < 6.5$ and seem to be having an important influence only for $y < 15$. For larger y spanwise velocities are controlled by larger scale ($\ell = 100$–150) eddies that dominate the flow outside the viscous wall region. Thus the signature of the $\lambda = 100$ eddies can be obtained from the spanwise variation of w at $y < 6.5$ or of v at $y = 30$–40. This can be rationalized from Figure 9. It is noted that the normal velocities associated with these eddies would be largest, and spanwise velocities would be the smallest, at a distance from the wall corresponding to the center of the eddy, $y = 20$–25. Using similar arguments, the contributions of these eddies to the w-velocity would be the largest and the contributions to the v-velocity would be smallest close to the wall.

The regions were v and w fluctuations are controlled by the

$\lambda = 100$ eddies can also be identifed by the spatial correlations in the flow direction. These show a range of y where the streamwise scale is a maximum and equal in extent to that defined by the uv correlation.

The spanwise correlations of u-velocity show scales consistent with the notion that $\lambda = 100$ eddies are creating these fluctuations. However, spatial correlations of u in the flow direction, unlike those for v and w, have a length which is twice that of the Reynolds stress producing eddies. This is consistent with the observation that these eddies appear intermittently, and suggests that the u-patterns created by them persist after they subside.

The association of Reynolds stress production in the viscous wall layer with approximately closed eddies having a spanwise dimension, on average, of 50 wall units has been suggested in numerous places in the literature, as discussed earlier.

The availability of computer simulations has enabled a number of researchers to explore this idea more directly in the last two years. A discussion of a few of these seems appropriate.

At the Zaric International Seminar on Wall-Turbulence, where this work was first presented, Robinson et al. (1988) gave an analysis of data from a computer simulation of a turbulent boundary-layer in which they suggested that there is a strong instantaneous spatial association between vortical structures and both quadrant 2 and quadrant 4 events. Figure 12 of their presentation shows this clearly. Guezennec et al. (1987) did a conditional average which detected quadrant 2 events at $y = 12$ and obtained results similar to what is shown in Figure 9a. Moin et al. (1987) used linear stochastic estimation to approximate the conditional vector fields in the y-z plane associated with high Reynolds stress producing events. These showed the stresses to be related to counterrotating eddies whose size increases with an increase of the distance of the detection point from the wall.

The main contribution of this paper is to document the connection of the production of Reynolds stress in the viscous wall region to eddy structure in a much more extensive and thorough manner.

Origin of the Reynolds stress eddies

Of considerable interest is the determination of the origin of the eddies in the viscous wall region that are creating Reynolds stresses. This paper presents only tentative (and, perhaps, speculative) answers to this question.

Results have been presented which have traced the change of eddies in the y-z plane backwards and forwards in the x-direction. These types of obervations indicate that the Reynolds stress producing structures quite often are associated upstream with very small scale eddies attached to the wall. This seems to be consistent with the suggestion of Townsend (1976) that the dominant structure in the wall region are double-cone eddies attached to the wall. Also, the suggested change of these eddies in the flow direction resembles the "vortical" structures identified by Robinson et al. (1988) as connected low pressure regions and, in fact, are probably the same.

It is now well documented that turbulence structures are convected long distances downstream, so that observations of the change of the turbulence at a fixed location with time, t, are approximately the same as the change observed in the flow direction, x, at a given time with x and t being connected by a convection velocity $U_c = x/t$. Therefore, the view taken in this paper in discussing the origin of the stress producing eddies is to look at changes in the flow direction. Thus, if the structures can be assumed to be quasi-steady in a frame of reference moving with a convection velocity then changes of eddy structures in the x-direction might be thought of as changes with flow time.

In this sense, it can be said that the eddies appear to originate in the viscous wall region. The only direct influence of the outer flow that was suggested from examining vector patterns is that large spanwise flows interact with the wall to produce small closed eddies in the y-z plane that are attached to the wall and that resemble separation bubbles.

Small eddies, such as these, are often observed to grow into attached eddies which, on average, have a dimension of $\ell \simeq 50$ and have their plane of rotation tilted upstream (backwards) at an angle of about 45° to the wall. Eventually these eddies detach from the wall and grow in size as they move away from the wall.

Relevance to previous laboratory studies

A comparison of the conceptual model and the results of correlations shows considerable consistency. This agreement is encouraging since a number of speculative ideas about the velocity field in the viscous wall layer, obtained from laboratory experiments, are confirmed. Some mention should, therefore, be made about results that were particularly gratifying or that were not anticipated.

It has often been suggested that Reynolds stress events are highly localized (Kim et al., 1977; Brodkey et al., 1974; Willmarth, 1975). The finding that they possess a streaky structure and that the eddies associated with them are somewhat elongated is, therefore, of interest.

The opportunity to relate scaling information obtained from correlation measurements or from conditional averages to observed instantaneous velocity fields has been most useful. Particular mention should be made of the direct connection of large Reynolds stresses with updrafts and downdrafts created by approximately closed eddies.

The tentative observation that stress producing eddies can often be traced backward in the flow direction to much smaller eddies that are attached to the wall could be most useful in understanding their origin. More important is the understanding of what governs the average size of the stress producing eddies, since their size probably determines the thickness of the viscous wall region, y_o. In a previous paper (Lyons et al., 1988) it was suggested the scaling adjusts so that the production of turbulence in the viscous wall region is almost in balance with the dissipation. It would be useful to use the type of detailed information provided by computer simulations to test this idea.

Acknowledgment

This work was supported by the Fluid Dynamics Program of the Office of Naval Research (N00014-82K0324) and by the Transport Phenomena Program of the National Science Foundation (NSF CBT 88-00980). J. B. M. acknowledges support from the Department of Energy under contract DE-FG02-88ER13919. We also acknowledge the support and facilities of the National Center for Supercomputer Applications at the University of Illinois, Urbana and at the Ballistics Research Laboratory, Aberdeen, Maryland.

Literature Cited

Adrian, R. J., P. Moin, and R. D. Moser, "Stochastic Estimation of Conditional Eddies in Turbulent Channel Flow," p. 7, *Studying Turbulent Using Numerical Simulation Databases*, Center for Turbu-

lence Research, NASA Ames Research Center, Report CTR-S87 (Dec. 1987).
Brodkey, R. S., J. M. Wallace, and H. Eckelmann, "Some Properties of Truncated Signals in Bounded Shear Flows," *J. Fluid Mech.*, **63,** 209 (1974).
Chapman, D. R., and G. D. Kuhn, "Two-Component Navier-Stokes Computational Model of the Viscous Sublayer Turbulence," AIAA Paper 81-1024, *Proc. AIAA CFD Conf.*, Palo Alto (1981).
Circelli, B., and J. B. McLaughlin, "Spatial Coherence in the Viscous Wall Region," *Physico-Chem. Hydrody.* **10,** 369 (1988).
Eckelman, L. D., "The Structure of Wall Turbulence and Its Relation to Eddy Transport," PhD Thesis, University of Illinois, Urbana (1971).
Finnicum, D. S., and T. J. Hanratty, "Effect of Favorable Pressure Gradients on Turbulent Boundary Layers," *AIChE J.*, **34,** 529 (1988).
Fortuna, G., "Effect of Drag-Reducing Polymers on Flow Near a Wall," PhD Thesis, University of Illinois, Urbana (1971).
Grant, H. L., "The Large Eddies of Turbulent Motion," *J. Fluid Mech.*, **4,** 149 (1958).
Guezennec, Y. G., U. Pionelli, and J. Kim. "Conditionally-Averaged Structures in Wall-Bounded Turbulent Flows," p. 263. *Study Turbulence Using Numerical Simulation Databases,* Center for Turbulence Research, NASA Ames Research Center, Report CTR-S87 (Dec. 1987).
Hanratty, T. J., "A Conceptual Model of the Viscous Wall Region," *Near Wall Turbulence,* Hemisphere, Washington, DC (1989).
Hatziavramidis, D. T., and T. J. Hanratty. "The Representation of the Viscous Wall Region by a Regular Eddy Pattern," *J. Fluid Mech.*, **95,** 655 (1979).
Hinze, J. O., *Turbulence,* 2nd ed, McGraw-Hill, New York (1975).
Hogenes, J. H. A., and T. J. Hanratty, "The Use of Multiple Wall Probes to Identify Coherent Flow Patterns in the Viscous Wall Region," *J. Fluid Mech.*, **124,** 363 (1982).
Johansson, A. V., P. H. Alfredsson, and J. Kim, "Shear-Layer Structures in Near Wall Turbulence," p. 237, *Studying Turbulence Using Numerical Simulation Databases,* Center for Turbulence Research, NASA Ames Research Center, Report CTR-S87 (Dec., 1987).
Kim, H. T., and R. P. Spalart, "Scalings of the Bursting Frequency in Turbulent Boundary Layers at Low Reynolds Numbers," *Phys. of Fluids,* **30,** 3326 (1987).
Kim, H. T., S. J. Kline, and W. C. Reynolds, "The Production of Turbulence Near a Smooth Wall in a Turbulent Boundary Layer," *J. Fluid Mech.*, **28,** 52 (1985).
Kim, J., P. Moin, and R. Moser, "Turbulence Statistics in Fully Developed Channel Flow at Low Reynolds Numbers," *J. Fluid Mech.*, **177,** 133 (1987).
Lee, M. K., L. D. Eckelman, and T. J. Hanratty, "Identification of Turbulent Wall Eddies Through the Phase Relation of the Components of the Fluctuating Velocity Gradient," *J. Fluid Mech.*, **66,** 17 (1974).
Lyons, S. L., "A Direct Numerical Simulation of Fully Developed Turbulent Channel Flow with Passive Heat Transfer," PhD Thesis, University of Illinois, Urbana (1989).
Lyons, S. L., C. Nikolaides, and T. J. Hanratty, "The Size of Turbulent Eddies Close to a Wall," *AIChE J.*, **34,** 938 (1988).
Marcus, P. S., "Simulation of Taylor-Couette Flow," *J. Fluid Mech.*, **146,** 45 (1984).
Moin, P., R. J. Adrian, and J. Kim, "Stochastic Estimation of Organized Structures in Turbulent Channel Flow," *Symp. on Turbulent Shear Flow, Toulouse* (Sept., 1987).
Niederschulte, M. A., "Turbulent Flow Through a Rectangular Channel," PhD Thesis, University of Illinois, Urbana (1989).
Nikolaides, C., K. K. Lau, and T. J. Hanratty, "A Study of the Spanwise Structure of Coherent Eddies in the Viscous Wall Region," *J. Fluid Mech.*, **130,** 91 (1983a).
Nikolaides, C., K. K. Lau, J. H. A. Hogenes, and T. J. Hanratty, "Structure of Turbulence Close to a Solid," *Annals of the New York Academy of Sciences,* **44,** 374 (1983b).
Nikolaides, C., "A Study of the Coherent Structures in the Viscous Wall Region of a Turbulent Flow," PhD Thesis, University of Illinois, Urban (1984).
Orszag, S. A., and L. C. Kells, "Transition to Turbulence in Plane Poiseuille and Plane Couette Flow," *J. Fluid Mech.*, **96,** 159 (1980).
Robinson, S. K., S. J. Kline, and P. R. Spalart, "Quasi-Coherent Structures in the Turbulent Boundary Layer: Part II Verification and New Information from a Numerically Simulated Flat-Plate Layer," Zoran P. Zaric International Seminar on Near-Wall Turbulence, Dubrovnik, Yugoslavia (May, 1988)
Sirkar, K. K., and T. J. Hanratty, "Relation of Turbulent Mass Transfer to a Wall at High Schmidt Numbers to the Velocity Field," *J. Fluid Mech.*, **44,** 589 (1970).
Smith, C. R., and S. P. Metzler, "The Characteristics of Low-Speed Streaks in the Near-Wall Region of a Turbulent Boundary Layer," *J. Fluid Mech.*, **129,** 25 (1929).
Townsend, A. A., *The Structure of Turbulent Shear Flow,* 2nd ed., Cambridge University Press (1976).
———, *The Structure of Turbulent Shear Flow,* p. 257, 2nd ed. Cambridge University Press, Cambridge (1976).
Tritton, D. J., "Some New Correlation Measurements in a Turbulent Boundary Layer," *J. Fluid Mech.*, **28,** 439 (1967).
Willmarth, W. W., *Advances in Fluid Mechanics,* **15,** 158, Academic Press (1975).

Manuscript received Apr. 18, 1989, and revision received Sept. 15, 1989.